



Influence of Industrial Wastes and Different Fluxes on Hot Metal Desulfurization Efficiency

ELTON VOLKERS DO ESPÍRITO SANTO ^{1,3}
SILAS GAMBARINE SOARES,¹ HEITOR CRISTO CLEM DE OLIVEIRA,¹
EDUARDO JUNCA,² FELIPE FARDIN GRILLO,¹
and JOSÉ ROBERTO DE OLIVEIRA¹

1.—Department of Metallurgical and Materials Engineering (PROPEMM), Federal Institute of Education, Science and Technology of Espírito Santo (IFES), Vitória 29040-780, Brazil. 2.—Department of Materials Science and Engineering (PPGCEM), Universidade do Extremo Sul Catarinense (UNESC), Criciúma 88806-000, Brazil. 3.—e-mail: elton.volkers@gmail.com

The use of recycled wastes and fluxing agents in hot metal desulfurizing mixtures aims to recover potential abilities from residues and to improve the reaction kinetics. Therefore, this work's aim is to propose calcitic lime partial replacement by limestone waste and slag from desulfurization in the Kambara Reactor. Likewise, it is proposed that fluorspar (CaF_2) is replaced by boron oxide (B_2O_3), sodalite and aluminum dross. Experimental tests were carried out in a resistance furnace at 1350°C in an inert atmosphere with constant stirring. Simulations were carried out with the FactSage software in order to obtain the phases present in each mixture at the working temperature. The most efficient mixtures formed a liquid phase above 20 wt.%, indicating that the dissolved CaO also desulfurizes hot metal. Limestone waste and the fluxes generated a positive effect on the desulfurization kinetics. It was possible to develop an empirical parameter called the global desulfurization factor (FG_{DeS}).

INTRODUCTION

Large quantities of solid wastes are generated annually in iron and steelmaking. In recent decades, efforts have been made to reintroduce these by-products as substitutes for the raw materials, in order to reduce production costs, to decrease slag generation, and to give them a more appropriate destination.¹

Kambara Reactor (KR) slag recycling as part of a hot metal desulfurizing mixture has been developed. However, the slag amount that can be recycled is limited due to the build-up of sulfur and the possibility of metal resulfurization. Nevertheless, recent studies have tested KR slag for this purpose.²

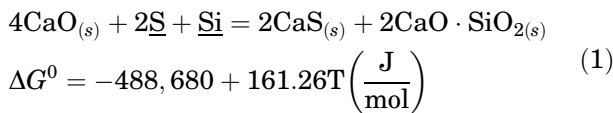
Nakai et al.³ developed a recycling method for the desulfurization of slag. The recycled slag had a 70% desulfurization capability compared with that of virgin flux. According to the authors, the slag silica content was responsible for this difference due to

the formation of solid phases. Tong et al.⁴ carried out studies on KR slag. According to them, about 56 wt.% of the KR slag can potentially be used as an iron-bearing raw material for the steelmaking process. The non-magnetic part was characterized and tested as desulfurization flux. Their results showed that the KR slag still has a desulfurization ability. Matsui et al.² reused previously desulfurized KR slag as a hot metal desulfurizing agent. Lime was completely replaced by KR slag, which resulted in a final sulfur content similar to that obtained with lime utilization (25 ppm, efficiency of 90%). The desulfurization rate in the first 4 min was slightly higher with lime utilization. The authors speculated that it is possible to recycle KR slag as a CaO source in desulfurization.

The limestone calcination for lime production in steel mills generates a particulate by-product called limestone waste. This residue is captured by the furnaces' dust filter collectors. Its chemical composition may vary depending on limestone type, kiln, fuel used, and the kiln operating parameters. It

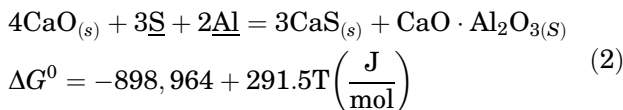
usually contains a high content of CaO.⁵ Studies using this residue as a substitute for lime in hot metal desulfurization are still difficult to find in the literature. However, Seshadri et al.⁶ and Vuolio et al.⁷ used calcium carbonate (CaCO₃) in their desulfurizing mixtures, and the increase in efficiency obtained was attributed to the increase in the reaction surface generated by the limestone decomposition and CO₂ release, which promotes greater bath stirring.

The formation of solid phases around the lime particles is one of the main controller mechanisms in hot metal desulfurization. Those solid products (CaS, 2CaO·SiO₂, and 3CaO·SiO₂) control the kinetic process since they hinder the sulfur mass transfer into lime.^{8,9} Equation 1 shows the desulfurization reaction with silicon:⁸



The effect of the solid phases on the desulfurization process can be decreased using a fluxing agent, since it dissolves the solid compounds into liquid slag. Fluorspar (CaF₂) has been reported in several papers as an effective fluxing material.^{8,10,11} However, the use of fluorspar presents both environmental and operational problems. Also, it is known that fluorspar increases the refractory wear.¹²

Grillo et al.¹³ determined that fluorspar is a better fluxing compound than sodalite, since the synthetic slag using sodalite contains a higher percentage of SiO₂. Other researchers have used mixtures of a CaO-Al system in the desulfurization process.^{10,14} The results indicated that the optimum percentage of aluminum was between 0.15 and 0.30 wt.%. The authors reported the formation of a liquid film of calcium aluminate around the lime particles, which improved the desulfurization rate. On the other hand, the excess of aluminum formed the solid phase of calcium aluminate that decreased the desulfurization rate.¹⁰ Mitsuo et al.¹⁴ reported that, when no aluminum was used, calcium silicates (2CaO·SiO₂, and 3CaO·SiO₂) having a high melting point and a low sulfur solubility were formed on the lime surface, and thereby sulfur transfer was retarded. When aluminum was added, a layer of CaO-Al₂O₃-FeO(Fe₂O₃)-based slag of low melting point and high sulfur solubility was formed on the lime surface, and sulfur could transfer through it and reach the lime. In this case, desulfurization efficiency was improved by 30% compared to no aluminum addition. Equation 2 displays the desulfurization reaction using aluminum:⁸



Yang et al.¹⁵ used aluminum dross as fluxing in the hot metal desulfurization process. The authors reached desulfurization efficiency between 80 and 90% after 40 min under calcium-aluminate top slag refining, without stirring. Moreira et al.¹⁶ investigated fluorspar, sodalite, aluminum dross, ulexite (NaCaB₅O₆(OH)₆·5(H₂O), which contains B₂O₃), and ilmenite as fluxing agents in hot metal desulfurization. The authors determined that a mixture containing 10.97 wt.% of ulexite reached 73.33% of desulfurization efficiency. On the other hand, the use of sodalite reached a desulfurization efficiency of 30.77%. In addition, the ulexite mixture presented lesser refractory wear than mixtures containing fluorspar and aluminum dross.

Wang et al.¹⁷ investigated the boron oxide effect instead of fluorspar in slags from the CaO-Al₂O₃ system in steel desulfurization by top slag without stirring. The authors mention that slags containing 4 wt.% of boron oxide presented better results than slags containing CaF₂, reaching final sulfur contents of between 20 and 40 ppm for a mass ratio of CaO/Al₂O₃ in the range of 1.5–7.0, while, in the case of CaF₂, the final sulfur content was between 50 and 80 ppm for a ratio of CaO/Al₂O₃ in the range of 1.2 and 3.0.

Several papers have demonstrated that the slags used in the hot metal desulfurization process present thermodynamic conditions to obtain lower the sulfur contents, which denotes that kinetics parameters (such as phases formed, percentage of solid and liquid phases, and viscosity) may limit the desulfurization reaction. Zhang et al.¹⁸ and Tong et al.¹⁹ studied the hot metal desulfurization kinetics by CaO-SiO₂-Al₂O₃-Na₂O-TiO₂ and CaO-Al₂O₃-SiO₂-MgO-TiO₂-Na₂O slags. The authors indicated that the sulfur mass transfer coefficient increases as the temperature increases and the slag viscosity decreases. Both the melting effect and the fluidity of the slag are enhanced when the temperature increases, and the controlling step is the mass transfer of sulfur in the slag phase. Concerning the stirring influence, Nakai et al.²⁰ argue that increasing the impeller rotation speed causes the reaction rate to increase, since it promotes particle dispersion, which enhances the reaction surface area and avoids particle aggregation.

The desulfurization rate is controlled by sulfur diffusion of the CaO particles (Eq. 3):²¹

$$-\frac{d[\%S]}{dt} = k' \times \left(\frac{A}{V_m} \right) \times ([\%S]_t - [\%S]_{eq}) \quad (3)$$

where A is the surface area between the CaO and the liquid metal (m²), k is the global coefficient of mass transportation (m/min), V is the hot metal volume, [%S]_t is the sulfur percentage at time t, and [%S]_{eq} is the equilibrium sulfur percentage.

Takahashi et al.²² investigated the role of solid lime and liquid slag during hot metal desulfurization. The reaction rate of solid CaO was low owing to

the formation of a solid interfacial layer. On the other hand, when solid lime and liquid slag act together, the desulfurization occurs by the liquid slag while the solid lime only supplies CaO for the liquid phase. In addition, the authors indicated that the dicalcium silicate phase decreases the reaction rate since it hinders the sulfur mass transfer while tricalcium aluminate does not hinder the mass transfer and hence increases the rate. Thus, the solid phases formed around the CaO particles (CaS, $2\text{CaO}\cdot\text{SiO}_2$, and $3\text{CaO}\cdot\text{SiO}_2$) hamper the mass transport of the desulfurization process, which decreases both the efficiency and the desulfurization rate. Therefore, studies of desulfurizing mixtures and phases formation are fundamental to a better understanding of the desulfurization process.

Broseghini et al.²³ and Pezzin et al.²⁴ studied dephosphorant and desulfurizing mixtures for the removal of phosphorus and sulfur from hot metal and steel by applying computational thermodynamics. The authors determined the slag properties such as the liquid and solid phases mass fractions, CaO and FeO activities in the liquid phase, liquid phase percentage, and slag viscosity, and used these data to develop expressions that were then related to dephosphorization and desulfurization efficiency.

Thus, the aim of this paper is to determine the desulfurization efficiency of mixtures containing sodalite, aluminum dross, and boron oxide, comparing them to fluorspar in order to replace it. Then, the partial replacement of lime by waste produced in steelmaking companies, such as limestone waste and slag from the desulfurization process in Kambara Reactor, was investigated. The phases present in the slag as well as the percentage of both solid and liquid phases were determined via FactSage 7.0 software. A new parameter to evaluate and predict the desulfurization efficiency of the mixtures has also been demonstrated and is called the desulfurization factor (F_{DeS}).

MATERIALS AND METHODS

Raw Materials Chemical Composition

The raw materials used in the experimental tests are the following: calcitic lime (C), limestone waste (L), KR slag (K), fluorspar (F), standard flux (SF), sodalite (S), boron oxide (B), and aluminum dross (A). The letters in parentheses represents the acronym for each one and will be used to name the desulfurization mixtures. See supplementary Table S-I to check the raw materials chemical composition (refer to online supplementary material). Calcitic lime, limestone waste, KR slag, and standard flux were provided by ArcelorMittal Tubarão, fluorspar and sodalite were provided by Tecnosulfur, hot metal was provided by Senai, and boron oxide and aluminum dross were produced at IFES. The particle size of all the materials was the same: between 0 and 2 mm.

The hot metal contained 94.6 wt.% of Fe, 4.77 wt.% of carbon, 0.042 wt.% of sulfur, 0.29 wt.% of silicon, 0.23 wt.% of manganese, and 0.060 wt.% of phosphorus.

Desulfurization Mixtures

The mixtures were prepared in order to study the calcitic lime replacement for alternative raw materials (group I) and to study the influence of different fluxes (group II) on the desulfurization efficiency. Thus, two groups of mixtures were defined.

Table I shows all the mixtures studied in this work. For group I mixtures, the standard flux was used as the fluxing agent, always at 12 wt.% to fix its influence on the process. The mixtures were prepared so that the CaO mass was practically the same. For mixtures from group II, there was emphasis on the fluorspar and boron oxide.

The standard mixture was C_{95}F_5 , containing 5 wt.% of fluorspar. It belongs to both groups. According to Niedringhaus and Fruehan¹⁰, a percentage in the range between 5 wt.% and 10 wt.% of fluorspar increases the desulfurization. To explain the mixtures' nomenclature, mixture C_{95}F_5 is taken as an example. The letter C represents the acronym of calcitic lime. The subscript number in the letter C (95) means the mass percentage of that raw material in the mixture, i.e., 95 wt.%.

Determination of the Phases Present in the Mixtures Heating

The simulation of the equilibrium phases was carried out by FactSage 7.0 software. The equilibrium phases of the mixtures and slags used the FactPS, Ftoxid, and FTMisc databases. The Pure Solids sub-database in the FactPS database was used to determine the solid phases formed in the mixtures. The SlagH sub-database in the FToxid database was used to determine the liquid phases formed in the mixtures containing fluorspar. The SlagA sub-database was used in mixtures without fluorspar. The FTMisc database was applied to determine the equilibrium sulfur percentage using the Liquid sub-database. All simulations occurred at 1350°C and 1 atm. Table II displays the input data used in the thermodynamic programming.

Desulfurization Tests

The desulfurization tests were accomplished in an electric resistance furnace. Figure 1a shows the schematic representation of the experimental apparatus, while Fig. 1b demonstrates the stirring mechanism used in the experimental tests.

The solid mass of hot metal was put into the MgO crucible (80 mm OD \times 70 mm ID \times 100 mm height) and heated up 1350°C in an electric resistance furnace (model MEV 1500/V ; FORTLAB). The tests were conducted under an argon (99.997% Ar) flow of

Table I. Proportion of materials used for mixtures from groups I and II

Group	Mixtures	Percentage (wt.%)							
		Calclitic Lime	Limestone Waste	KR Slag	Fluorspar	Standard Flux	Sodalite	Boron Oxide	Aluminum Dross
I, II	C ₉₅ F ₅	95	–	–	5	–	–	–	–
I	C ₈₈ SF ₁₂	88	–	–	–	12	–	–	–
I	C ₈₀ L ₈ SF ₁₂	80	8	–	–	12	–	–	–
I	C ₈₂ K ₆ SF ₁₂	82	–	6	–	12	–	–	–
I	C ₇₄ L ₈ K ₆ SF ₁₂	74	8	6	–	12	–	–	–
I	C ₇₃ L ₁₅ SF ₁₂	73	15	–	–	12	–	–	–
II	C ₈₁ L ₈ K ₆ B ₅	81	8	6	–	–	–	5	–
II	C ₆₉ L ₁₅ K ₆ S ₅ F ₅	69	15	6	5	–	5	–	–
II	C ₆₉ L ₁₅ K ₆ S ₅ B ₅	69	15	6	–	–	5	5	–
II	C ₆₇ L ₁₅ K ₆ S ₆ A ₆	67	15	6	–	–	6	–	6
II	C ₆₇ L ₁₅ K ₆ S ₄ A ₄ F ₄	67	15	6	4	–	4	–	4
II	C ₆₇ L ₁₅ K ₆ S ₄ A ₄ B ₄	67	15	6	–	–	4	4	4

4NI/min to prevent the metal oxidation. After the metal melting, the initial sample was taken (time zero) using a vacuum sampler, and the desulfurization mixture was added to the liquid metal using a stainless steel tube. The mechanical stirring speed was 500 rpm. This speed was calculated in order to obtain the same stirring energy as industrial reactors. It started immediately after mixture charging, as well as the measured reaction time. Then, aliquots were removed from the bath at 3, 6, 9, 12, 15, and 25 min. Finally, the sulfur content was determined by infrared analysis through direct combustion of the samples in a LECO model CS-444 LS.

Desulfurization Efficiency

The desulfurization efficiency (Eq. 4) was determined by the initial [%S_i] and final [%S_f] sulfur content.

$$\eta(\%) = \frac{[\%S_i] - [\%S_f]}{[\%S_i]} \times 100 \quad (4)$$

Determination of the Desulfurization Factor

Equation 3 demonstrated that the desulfurization is controlled by the sulfur mass transport to the lime. In addition, the solid phases formed around the lime particles hinder the mass transport. The desulfurization factor (F_{DeS}) was elaborated to investigate the influence of those solid phases on desulfurization efficiency. Thus, increasing the F_{DeS} parameter also increases the desulfurization efficiency (for the same conditions of temperature and stirring). The F_{DeS} will be determined using the phases obtained in the thermodynamic simulation.

RESULTS AND DISCUSSION

Figure 2 displays the sulfur variations against time for mixtures from groups I and II, as well as their desulfurization efficiencies after 25 min. Table III displays the phases formed at 1350°C by Factsage software for both groups. The results are presented and discussed in the following topics for each one.

It can be seen from Fig. 2 and Table III that the group II mixtures had a greater desulfurization efficiency. Table III shows that these mixtures had a percentage of liquid phase above 20 wt.% (except for C₉₅F₅). The results and discussion are presented in the following topics for each group.

Influence of Lime Partial Replacement (Group I)

From Fig. 2a, it can be seen that mixture C₉₅F₅ presented the highest value of desulfurization efficiency (80.70%). It can also be seen that a decrease of the desulfurization efficiency occurred, decreasing the percentage of calcitic lime in the mixture composition. The mixtures containing limestone waste (C₈₀L₈SF₁₂ and C₇₃L₁₅SF₁₂) reached values of desulfurization efficiency of 75.56 and 76.00%, respectively. This was due to the decomposition of limestone into CaO and CO₂, which caused stirring in the bath, increasing the reaction velocity. On the other hand, the mixture C₇₄L₈K₆SF₁₂ (containing both limestone waste and KR slag) reached a desulfurization efficiency of 65.12%, the lowest one. Comparing it with the C₈₀L₈SF₁₂ mixture shows that exchanging 6% of calcitic lime for KR slag causes a decrease in efficiency. At the same time, a comparison between the C₇₄L₈K₆SF₁₂ and C₇₃L₁₅SF₁₂ mixtures indicates that replacing 6% of limestone waste for KR slag also decreases the efficiency. In other words, it can be said that calcitic

Table II. Chemical composition of the mixtures used as input data in the thermodynamic programming

Mixture	Chemical composition (wt.%)														Mass (g)	
	CaO	SiO ₂	Al ₂ O ₃	CaF ₂	Fe ₂ O ₃	MgO	K ₂ O	FeO	B ₂ O ₃	MnO	Na ₂ O	S	C	P		Al
C ₉₅ F ₅	15.35	0.20	0.05	0.59	0.05	0.03	0.01	0.00	0.00	0.00	0.00	0.01	0.00	0.01	0.00	16.31
C ₈₈ SF ₁₂	14.21	0.62	0.44	0.00	0.01	0.06	0.06	0.00	0.00	0.01	0.51	0.01	0.00	0.01	0.30	16.25
C ₈₀ L ₈ SF ₁₂	14.91	0.65	0.47	0.00	0.01	0.07	0.06	0.00	0.00	0.01	0.54	0.01	0.00	0.01	0.32	17.06
C ₈₂ K ₆ SF ₁₂	13.56	0.69	0.48	0.00	0.01	0.08	0.06	0.45	0.00	0.02	0.51	0.03	0.02	0.01	0.30	16.20
C ₇₄ L ₈ K ₆ SF ₁₂	14.21	0.73	0.50	0.00	0.01	0.08	0.06	0.47	0.00	0.02	0.54	0.03	0.02	0.01	0.32	16.99
C ₇₃ L ₁₅ SF ₁₂	15.54	0.69	0.49	0.00	0.01	0.07	0.07	0.00	0.00	0.01	0.56	0.01	0.00	0.01	0.33	17.79
C ₈₁ L ₈ K ₆ B ₅	15.60	0.19	0.05	0.00	0.01	0.05	0.00	0.48	0.87	0.01	0.00	0.03	0.02	0.01	0.00	17.31
C ₆₉ L ₁₅ K ₆ S ₅ F ₅	15.15	0.76	0.30	0.64	0.08	0.06	0.07	0.49	0.00	0.01	0.12	0.03	0.02	0.01	0.00	17.76
C ₆₉ L ₁₅ K ₆ S ₅ B ₅	15.12	0.66	0.25	0.00	0.05	0.06	0.06	0.49	0.89	0.01	0.13	0.03	0.02	0.01	0.00	17.77
C ₆₇ L ₁₅ K ₆ S ₆ A ₆	14.84	0.77	0.96	0.00	0.05	0.06	0.07	0.49	0.00	0.01	0.15	0.03	0.02	0.01	0.39	17.85
C ₆₇ L ₁₅ K ₆ S ₄ A ₄ F ₄	14.83	0.66	0.69	0.51	0.07	0.06	0.06	0.49	0.00	0.01	0.10	0.03	0.02	0.01	0.26	17.80
C ₆₇ L ₁₅ K ₆ S ₄ A ₄ B ₄	14.88	0.58	0.65	0.00	0.04	0.06	0.05	0.49	0.72	0.01	0.10	0.03	0.02	0.01	0.26	17.90

lime and limestone waste are more appropriate than KR slag for desulfurization.

The mixtures C₈₂K₆SF₁₂ and C₇₄L₈K₆SF₁₂ containing KR slag reached the lowest desulfurization efficiencies (67.57 and 65.12%, respectively), since that residue presented only 36 wt.% of CaO, a high content of FeO (46 wt.%), and sulfur. According to Iwamasa and Fruehan²⁵, the increase in FeO content in the slag promotes a decrease in the desulfurization rate, since the equilibrium sulfur content increases. The oxygen potential at the metal/slag interface is greater as the FeO content increases. In this case, the driving force of the desulfurization reaction decreases. Mathematically, this is shown in Eq. 3. Figure 2a also demonstrates that the addition of 5 wt.% of fluorspar was more efficient than the addition of 12 wt.% of standard flux.

From Table III, it can be seen that the most efficient mixture, C₉₅F₅, was the one with the lowest solid phase formation (except for CaO). At the same time, the mixtures with lower efficiencies were those with the highest solid phase formation, mainly tricalcium silicate (3CaO·SiO₂). McFeaters and Fruehan⁸ indicated that this phase hinders the reaction kinetics by precipitating around the CaO particles, delaying sulfur diffusion. The mixtures with the lower efficiencies are those that also have the highest liquid phase amount and the lowest solid CaO amount. In these cases, part of the CaO particles form the liquid slag and the solid phases, decreasing the amount available to react with the sulfur. In addition, the equilibrium sulfur content has no relationship to efficiency.

Fluxes Influence (Group II)

From Fig. 2b it can be seen that the mixture C₆₉L₁₅K₆S₅B₅ presented the highest desulfurization efficiency. The mixtures C₆₉L₁₅K₆S₅B₅, C₆₇L₁₅K₆S₄A₄B₄, C₆₇L₁₅K₆S₄A₄F₄, and C₆₇L₁₅K₆S₆A₆ were more efficient than the mixture containing calcitic lime and fluorspar, which suggests that the use of those fluxing materials was more effective than just using fluorspar. In addition, this high efficiency was also due to the use of 15 wt.% of limestone waste, which contributes to the reaction kinetics, as has been previously discussed.

Comparing the mixture C₆₉L₁₅K₆S₅F₅ with C₆₉L₁₅K₆S₅B₅ and C₆₇L₁₅K₆S₄A₄F₄ with C₆₇L₁₅K₆S₄A₄B₄, it was noted that the use of boron oxide reached better results for desulfurization efficiency than mixtures containing fluorspar. This indicates that the boron oxide is more effective in dissolving the solid phases formed around the CaO particles than fluorspar, since the boron oxide decreases both the melting temperature and the viscosity of the desulfurizing slags, as reported by Wang et al.¹⁷.

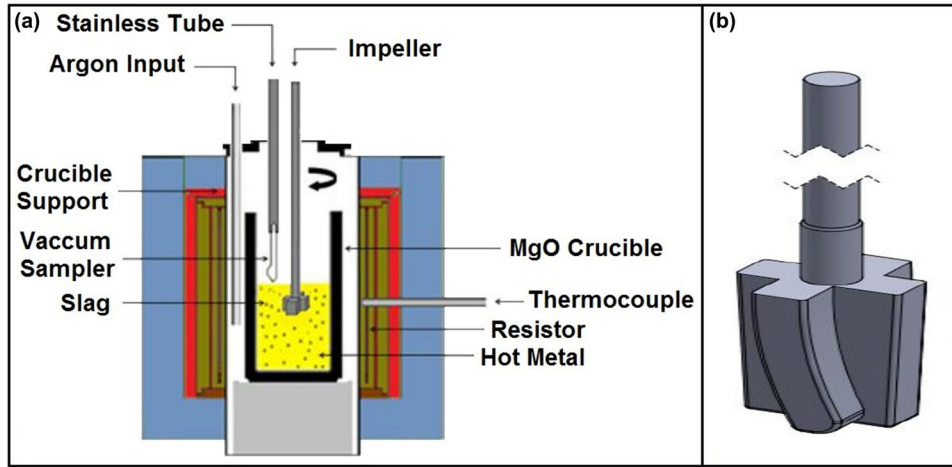


Fig. 1. (a) Schematic of the experiments; (b) mechanical stirrer.

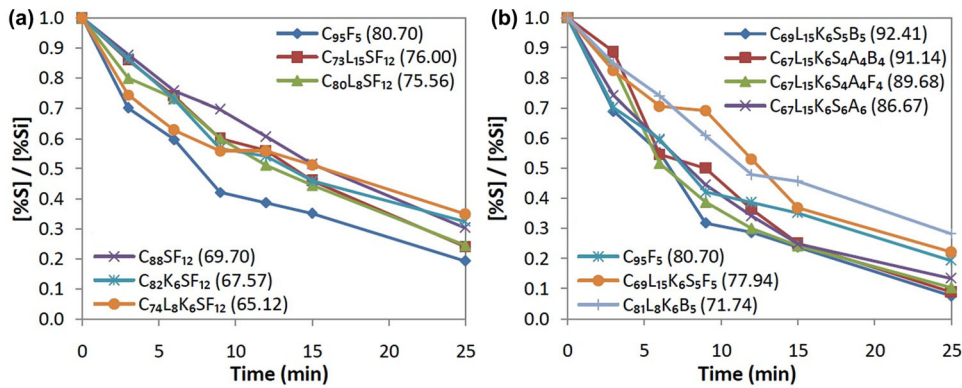


Fig. 2. Sulfur variation [%S]/[%Si] against time. (a) Mixtures from group I; (b) mixtures from group II.

Table III. Phases formed in mixtures simulation for mixtures from groups I and II

Group	Mixture	%Liq	%Sol	% Solid phases					%Seq	η (%)
				CaO	CaS	MgO	3CaO·SiO ₂	3CaO·B ₂ O ₃		
II	C ₆₉ L ₁₅ K ₆ S ₅ B ₅	31.45	68.56	67.71	0.29	0.00	0.00	0.00	2.17E-05	92.41
II	C ₆₇ L ₁₅ K ₆ S ₄ A ₄ B ₄	33.87	66.13	60.49	0.00	0.00	5.64	0.00	2.14E-05	91.14
II	C ₆₇ L ₁₅ K ₆ S ₄ A ₄ F ₄	28.78	71.22	70.88	0.34	0.00	0.00	0.00	2.15E-05	89.68
II	C ₆₇ L ₁₅ K ₆ S ₆ A ₆	28.58	70.76	70.76	0.00	0.00	0.00	0.00	2.15E-05	86.67
I, II	C ₉₅ F ₅	8.60	91.40	90.99	0.10	0.19	0.00	0.00	2.16E-05	80.79
II	C ₆₉ L ₁₅ K ₆ S ₅ F ₅	23.61	76.39	75.69	0.36	0.13	0.00	0.00	2.22E-05	77.94
II	C ₈₁ L ₈ K ₆ B ₅	11.94	88.06	76.24	0.36	0.00	0.00	9.48	2.21E-05	71.74
I	C ₇₃ L ₁₅ SF ₁₂	14.85	85.15	74.73	0.20	0.00	7.13	0.00	2.01E-05	76.00
I	C ₈₀ L ₈ SF ₁₂	15.48	84.52	77.06	0.18	0.00	7.06	0.00	1.93E-05	75.56
I	C ₈₈ SF ₁₂	16.25	83.75	76.26	0.16	0.00	6.96	0.00	1.73E-05	69.70
I	C ₈₂ K ₆ SF ₁₂	17.71	82.29	69.71	0.34	0.00	11.41	0.00	2.00E-05	67.57
I	C ₇₄ L ₈ K ₆ SF ₁₂	17.02	82.98	69.94	0.36	0.00	11.09	0.00	2.08E-05	65.12

The mixture C₆₇L₁₅K₆S₆A₆, containing sodalite and aluminum dross, reached a desulfurizing efficiency of 86.67%. On the other hand, regarding the mixture with the lowest efficiency (C₈₁L₈K₆B₅), it is noticed that even with boron oxide present probably

the low limestone waste amount (8 wt.%) impacted the process kinetics compared to the others. It is also noticed that the presence of 6 wt.% of KR slag in the mixtures with efficiencies higher than 85% has not affected their desulfurization ability, what

make its use feasible without compromising the process.

Table III shows that the mixtures $C_{69}L_{15}K_6S_5B_5$ and $C_{67}L_{15}K_6S_4A_4B_4$ reached a desulfurization efficiency of 92.41% and 91.14%, respectively, even containing a smaller solid CaO percentage. In addition, there was practically no solid phase formation in the first one (except for CaO). Otherwise, the mixture $C_{67}L_{15}K_6S_4A_4B_4$ formed 5.64 wt.% of $3CaO \cdot SiO_2$, which suggests that this phase may not have affected the desulfurization efficiency, since the content of the liquid phase was the highest among all the mixtures (33.87 wt.%). This indicates that the desulfurization also occurred by CaO dissolved in the liquid phase, since its activity is 1 (in all cases there is solid CaO formation; that is, the liquid is saturated with CaO). It is also noted there are four mixtures with a high desulfurization efficiency (above 85%) containing a liquid phase percentage higher than 25 wt.%, indicating that liquid phases present in an amount above this value increase the desulfurization efficiency, since the liquid-liquid reaction favors the mass transport of sulfur. The mixture $C_{81}L_8K_6B_5$ presented the lowest desulfurization efficiency since it has a low limestone waste content. In addition, it formed 9.48 wt.% of $3CaO \cdot B_2O_3$, which decreased the CaO content available to the desulfurization reaction.

Determination of the Desulfurization Factor (F_{DeS})

Equation 3 shows that the hot metal desulfurization reaction depends on the sulfur mass transport to the lime. In addition, the solid phases formed around the lime particles hinder the mass transport. As the desulfurization occurs by a direct reaction between the CaO particles and sulfur in hot metal, it should be considered that the CaO particles are effectively available to react. The presence of solid phases such as calcium sulfide and calcium silicates hampers the reaction. Thus, it is proposed that the efficiency depends on the free lime percentage minus the solid phases sum, while it is expected that the greater the solid phases amount, the lower the lime available to react, and, hence, the lower the efficiency. Based on this concept and the phases obtained with the FactSage software, a new parameter can be determined. It was called the desulfurization factor (F_{DeS}) and was related to the desulfurization efficiency. Increasing this factor also increases the mixture efficiency, at the same temperature and stirring conditions. Table III shows the formation of CaS and $3CaO \cdot SiO_2$ in the mixtures studied in this work. Such phases are reported in the literature as being formed around the CaO particles. Therefore, F_{DeS} is defined according to Eq. 5:

$$F_{DeS} = (\%CaO_S) - (\%3CaO \cdot SiO_2 + \%CaS) \quad (5)$$

The mixtures used in this paper were produced with different raw materials. In this way, the analysis of the desulfurization factor occurred in groups similar to each other. This was due to the chemical composition of F_{DeS} being considered. In addition, the factors that affect the reaction kinetics cannot be different between the mixtures. All materials used in the tests have the same particle size range, between 0 and 2 mm. In the present work, limestone waste and KR slag are inputs that affect the desulfurization kinetics. The first was used in most tests in different proportions (15 wt.%, 8 wt.%, and 0 wt.%). Since the carbonate decomposition affects the process kinetics, mixtures with different levels of limestone waste cannot be compared by the desulfurization factor. Also, mixtures with different percentages of KR slag cannot be compared since the CaO is present in other phases, such as CaS and $3CaO \cdot SiO_2$, as the KR slag is a waste. In addition, the CaO reactivity in the KR slag is probably less than the calcitic lime since that may be sintered or hydrated. Therefore, the mixtures were grouped with the same levels of both limestone waste and KR slag to avoid the influence of the inputs on the desulfurization factor. Thus, three sets of samples were defined:

- Group 1 – without limestone waste and KR slag: $C_{95}F_5$ and $C_{88}SF_{12}$;
- Group 2 – 8 wt.% of limestone waste and 6 wt.% of KR slag: $C_{81}L_8K_6B_5$ and $C_{74}L_8K_6SF_{12}$;
- Group 3 – 15 wt.% of limestone waste and 6 wt.% of KR slag: $C_{69}L_{15}K_6S_5F_5$, $C_{69}L_{15}K_6S_5B_5$, $C_{67}L_{15}K_6S_4A_4F_4$, $C_{67}L_{15}K_6S_4A_4B_4$, and $C_{67}L_{15}K_6S_6A_6$.

The mixtures $C_{73}L_{15}SF_{12}$, $C_{80}L_8SF_{12}$, and $C_{82}K_6SF_{12}$ were not classified in any group, and the desulfurization factor was not calculated. Equation 5 was used to determine the desulfurization factor for groups 1 and 2. Table IV shows the F_{DeS} and desulfurization efficiency for them.

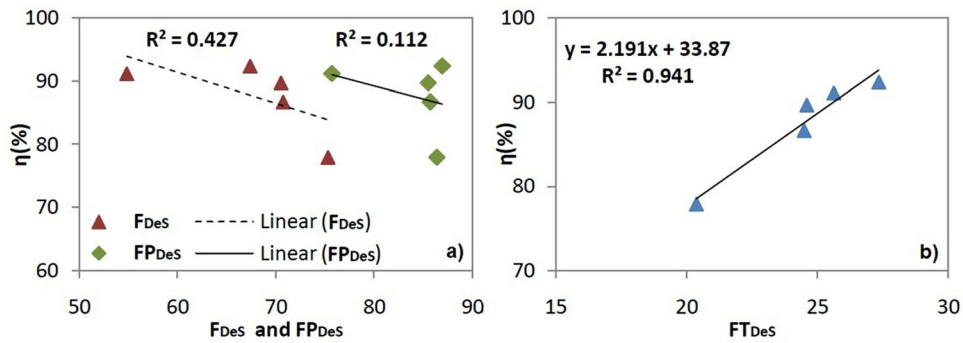
It can be noted from Table IV that increasing the F_{DeS} also increases the desulfurization efficiency in both groups. Therefore, Eq. 5 can be applied to evaluate the mixtures' efficiency with the characteristics of groups 1 and 2.

Table III demonstrates that the mixtures from group 3 formed the liquid phase between 23.61 and 33.87 wt.%. In addition, increasing the content of liquid slag decreases the percentage of solid CaO, since part of the CaO dissolves in the liquid, and the desulfurization factor (Eq. 5) also decreases. However, the desulfurization efficiency of the mixtures from group 3 (between 77.94 and 92.41%) was higher than the efficiency of groups 1 and 2, which disagrees with the decreasing of the desulfurization factor.

The greater efficiency of the mixtures from group 3 may indicate that the CaO in the liquid part can desulfurize hot metal, once the CaO activity in the

Table IV. Desulfurization factor (F_{DeS} , FP_{DeS} e FT_{DeS}) and desulfurization efficiency for mixtures from groups 1, 2 and 3

Group	Mixture	%CaO _L	N_{Liq}	F_{DeS}	FP_{DeS}	FT_{DeS}	$\eta(\%)$
1	C ₉₅ F ₅	—	—	90.89	—	—	80.70
1	C ₈₈ SF ₁₂	—	—	69.14	—	—	69.70
2	C ₈₁ L ₈ K ₆ B ₅	—	—	75.88	—	—	71.74
2	C ₇₄ L ₈ K ₆ SF ₁₂	—	—	58.49	—	—	65.12
3	C ₆₉ L ₁₅ K ₆ S ₅ B ₅	19.55	0.3145	67.42	86.97	27.35	92.41
3	C ₆₇ L ₁₅ K ₆ S ₄ A ₄ B ₄	20.89	0.3387	54.85	75.74	25.65	91.14
3	C ₆₇ L ₁₅ K ₆ S ₄ A ₄ F ₄	14.97	0.2878	70.54	85.51	24.61	89.68
3	C ₆₇ L ₁₅ K ₆ S ₆ A ₆	15.00	0.2858	70.76	85.75	24.51	86.67
3	C ₆₉ L ₁₅ K ₆ S ₅ F ₅	11.06	0.2361	75.33	86.39	20.40	77.94

Fig. 3. Relationship between the desulfurization factor versus efficiency for group 3 mixtures. (a) F_{DeS} and FP_{DeS} , (b) FT_{DeS} .

liquid slag is 1. However, the desulfurization for mixtures containing up to 20 wt.% of liquid phases occurs predominantly by solid CaO.

Thus, Equation 6 demonstrates a new desulfurization factor, called partial desulfurization factor (FP_{DeS}), proposed for mixtures with percentage of liquid phase higher than 20 wt.%. FP_{DeS} considers the liquid CaO percentage (%CaO_L).

$$FP_{DeS} = \%CaO_S + \%CaO_L - (\%3CaO \cdot SiO_2 + \%CaS) \quad (6)$$

Figure 3a presents the graphs that relate the desulfurization factor (F_{DeS} and FP_{DeS}) with the efficiency of mixtures from group 3.

Figure 3a shows a low coefficient of determination ($R^2 = 0.427$ and 0.112) between the desulfurization factor (F_{DeS} and FP_{DeS}) and desulfurization efficiency for mixtures from group 3. A tendency to a decrease in the desulfurization efficiency with an increase of the desulfurization factor can also be seen. Such results indicate that the Eqs. 5 and 6 should not be used to determine the desulfurization factor of the mixtures from group 3.

This result prompted the search for a model that is representative for mixtures with such characteristics. Table III demonstrates that the mixtures from group 3 presented a content of liquid phase above 20 wt.%. Thus, a new term was added to the FP_{DeS} . By multiplying the FP_{DeS} by the mass

fraction of liquid (N_{Liq}), it was possible to obtain the desulfurization factor for mixtures with liquid formation above 20wt.%, called the total desulfurization factor (FT_{DeS}). Equation 7 presents this new expression.

$$FT_{DeS} = [\%CaO_S + \%CaO_L - (\%3CaO \cdot SiO_2 + \%CaS)] \times N_{Liq} \quad (7)$$

Table IV displays the values of the three models for the mixtures from group 3, as well as the values of the mass fraction of liquid (N_{Liq}) and the liquid CaO content (%CaO_L).

Figure 3b shows the linear regression between FT_{DeS} and the desulfurization efficiency.

Table IV and Figure 3b show that increasing the FT_{DeS} also increases the desulfurization efficiency. Therefore, it can be confirmed that the higher the FT_{DeS} value, the more efficient the mixture.

The coefficient of determination of 0.941 indicates that 94.10% of the efficiency variation can be explained by the variation of the FT_{DeS} . This shows that the linear regression model presented can predict the desulfurization efficiency for this type of mixtures. Thus, efficiency can be obtained by the expression of Eq. 8.

$$\eta(\%) = 2.191 \times (FT_{DeS}) + 33.87 \quad (8)$$

It is important to note that this model applies only to mixtures with the same characteristics as those used in this work and under the same experimental conditions.

Although the mixtures from group 3 are more efficient than those from groups 1 and 2, their FT_{DeS} values are lower than the F_{DeS} values shown in Table IV, a fact that is not in agreement with the purpose of creating this parameter, that is, increasing the desulfurization factor also increases the mixture efficiency. Considering that a standardization of the desulfurization factor expression must be made, that is, that the mixture with the highest factor will always result in greater efficiency, a general model for mixtures with liquid phase formation above or below 20 wt.% is proposed. The global desulfurization factor (FG_{DeS}) is presented by Eq. 9.

$$FG_{DeS} = [\%CaO_S + \%CaO_L - (\%3CaO \cdot SiO_2 + \%CaS)] \times N_{Liq} \times k \tag{9}$$

For %Liquid < 20 → $k = 1$,

$N_{Liq} = 1$ and

$\%CaO_L = 0$;

For %Liquid > 20 → $k = 4.24$,

$N_{Liq} =$ Liquid mass fraction and

$\%CaO_L = \%CaO$ of the liquid phase

where k is the desulfurization constant, which adjusts the values of the desulfurization factor and was obtained empirically. For the mixtures studied in this work, the value of k is equal to 4.24.

Thus, the higher the FG_{DeS} value, the greater the desulfurization efficiency for all the mixtures, as can be seen in Fig. 4.

The FG_{DeS} values presented in the graph above correspond to those obtained by the models in Eq. 9, which generalize the desulfurization factor for mixtures with a quantity of liquid below and above 20 wt.%.

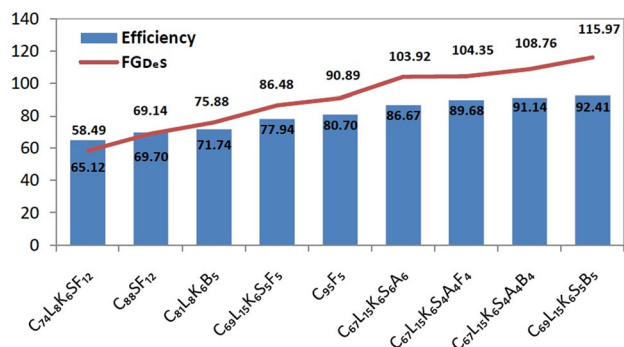


Fig. 4. Values of desulfurization efficiency and FG_{DeS} for the mixtures studied in this paper

CONCLUSION

Increasing the percentage of limestone waste favors the desulfurization process due to kinetic factors caused by $CaCO_3$ decomposition, which indicates that this waste can be used to replace part of the lime. On the other hand, the use of KR slag has decreased the desulfurization efficiency, which demonstrates that little content of this waste can be used. However, when this residue is combined with the fluxes, it has not affected the desulfurization ability. The combined use of fluxing materials in the mixtures generated greater desulfurization efficiency. The comparison between fluor-spar and boron oxide showed that the latter promoted better results, with the $C_{69}L_{15}K_6S_5B_5$ mixture reaching the highest efficiency (92.41%). A liquid phase content higher than 20 wt.% increased the desulfurization efficiency. The expression that determines the global desulfurization factor (FG_{DeS}) is:

$$FG_{DeS} = [\%CaO_S + \%CaO_L - (\%3CaO \cdot SiO_2 + \%CaS)] \times N_{Liq} \times k$$

ACKNOWLEDGEMENTS

Thanks to Coordenação de Aperfeiçoamento de Pessoal de nível Superior, Fundação de Amparo à Pesquisa e Inovação do Espírito Santo, Conselho Nacional de Desenvolvimento Científico e Tecnológico, and Programa de Pós-Graduação em Engenharia Metalúrgica e de Materiais for technical and laboratory support.

CONFLICT OF INTEREST

On behalf of all authors, the corresponding author states that there is no conflict of interest.

SUPPLEMENTARY INFORMATION

The online version contains supplementary material available at <https://doi.org/10.1007/s11837-021-04673-3>.

REFERENCES

- H.M. Ahmed, E.A. Mousa, M. Larsson, and N.N. Viswanathan, *Ironmaking and Steelmaking Processes - Greenhouse Emissions, Control, and Reduction*, ed. P. Cavaliere (Lecce: Springer, 2016), p. 101.
- A. Matsui, Y. Uchida, N. Kikuchi, and Y. Miki, *ISIJ Int.* 57, 1012. (2017).
- Y. Nakai, N. Kikuchi, M. Iwasa, S. Nabeshima, and Y. Kishimoto, *Steel Res. Int.* 80, 727. (2009).
- Z. Tong, G. Ma, X. Cai, Z. Xue, W. Wang, and X. Zhang, *Waste Biomass Valorization* 7, 1. (2016).

5. M.A. Latif, S. Naganathan, H.A. Razak, and K.N. Mustapha, *Procedia Eng.* 125, 780. (2015).
6. V. Seshadri, A.C. Silva, and I.A. Silva, *Mater. Manuf. Processes* 17, 693. (2002).
7. T. Vuolio, V.V. Visuri, S. Tuomikoski, T. Paananen, and T. Fabritius, *Metall. Mater. Trans B* 49, 2692. (2018).
8. L.B. McFeaters, and R.J. Fruehan, *Metall. Mater. Trans. B* 24B, 441. (1993).
9. D. Lindström, and D. Sichen, *Metall. Mater. Trans. B* 46, 83. (2015).
10. J.C. Niedringhaus, and R.J. Fruehan, *Metall. Mater. Trans. B* 19, 261. (1988).
11. E. Oktay, and R.J. Fruehan, *Steel Res. Int.* 66, 93. (1995).
12. T. W. Miller, J. Jimenez, A. Sharan, and D. A. Goldstein, *The Making, Shaping and Treating of Steel: Steelmaking and Refining Volume*, ed. R. J. Fruehan (Pittsburgh: The AISE Steel Foundation, 1998), p. 475.
13. F.F. Grillo, R.A. Sampaio, J.F. Viana, D.C.R. Espinosa, and J.R. Oliveira, *REM. Rev. Esc. Minas* 66, 461. (2013).
14. T. Mitsuo, T. Shoji, Y. Hatta, H. Ono, H. Mori, and T. Kai, *Trans. Jpn. Inst. Met.* 23, 768. (1982).
15. Y. Yang, P. Wu, G. Men, and A. McLean, *High Temp. Mater. Proc.* 31, 519. (2012).
16. A.S.B. Moreira, C.A. Silva, and I.A. Silva, *REM. Int. Eng. J.* 71, 261. (2018).
17. H. Wang, T. Zhang, H. Zhu, G. Li, Y. Yan, and J. Wang, *ISIJ Int.* 51, 702. (2011).
18. K.H. Zhang, Y.L. Zhang, and T. Wu, *J. Iron Steel Res. Int.* 26, 1041. (2018).
19. Z. Tong, J. Qiao, and X. Jiang, *ISIJ Int.* 57, 245. (2017).
20. Y. Nakai, I. Sumi, H. Matsuno, N. Kikuchi, and Y. Kishimoto, *ISIJ Int.* 50, 403. (2010).
21. J.Y. Choi, D.J. Kim, and H.G. Lee, *ISIJ Int.* 41, 218. (2001).
22. K. Takahashi, K. Utagawa, H. Shibata, S.Y. Kitamura, N. Kikuchi, and Y. Kishimoto, *ISIJ Int.* 52, 10. (2012).
23. F.C. Broseghini, H.C.C. Oliveira, S.G. Soares, F.F. Grillo, and J.R. Oliveira, *REM. Int. Eng. J.* 71, 217. (2018).
24. R.O. Pezzin, A.P.L. Berger, F.F. Grillo, E. Junca, H.S. Furtado, and J.R. Oliveira, *J. Mater. Res. Technol.* 9, 838. (2020).
25. P.K. Iwamasa, and R.J. Fruehan, *Metall. Mater. Trans. B* 28, 47. (1997).

Publisher's Note Springer Nature remains neutral with regard to jurisdictional claims in published maps and institutional affiliations.